Research Article

The liquid environment effect on photoluminescence properties of carbon nanoparticles prepared by laser ablation method in liquids with possible biocompatibility applications

Fatemeh Kazemizadeh [a], Samad Moemen Bellah [a,b*], and Rasoul Malekfar [a]

a Department of Physics, Faculty of Basic Sciences, Tarbiat Modares University, P.O. Box 14115-175, Tehran 14117-13116, Islamic Republic of Iran
b Department of Process Modeling and Control, Faculty of Engineering, Iran Polymer and Petrochemical Institute, Tehran 14977-13115, Islamic Republic of Iran

***Corresponding author, Email: s.moemen@ippi.ac.ir**

DOI: 10.30495/ijbbe.2023.1980332.1022

ABSTRACT

Received: Feb. 15, 2023, Revised: Apr. 25, 2023, Accepted: Jun. 21, 2023, Available Online: Jun. 29, 2023

Fluorescent carbon nanoparticles (CNPs) were prepared by nanosecond laser ablation of graphite powder in liquid. The effect of the liquid medium on photoluminescence (PL) efficiency and wavelength range were studied experimentally. Four solvents, polyethylene glycol, diethanolamine, diethylamine, and ethylenediamine were used as liquid platforms in the synthesis process. Analyzing the chemical components and optical spectral characterization of CNPs was carried out by attenuated total reflection Fourier-transform infrared (ATR-FTIR) spectroscopy and photoluminescence (PL) spectroscopy, respectively. Moreover, the size of CNPs was estimated by using dynamic light scattering (DLS) measurements. Liquid components are determined to be a key factor affecting PL properties and nanoparticle size. The results are valuable in practical applications.

KEYWORD

carbon nanoparticle; fluorescent; laser ablation in liquids; photoluminescence; biocompatibility

I. INTRODUCTION

Fluorescent carbon nanoparticle (CNP), a new class of carbon allotropes, is an excellent potential nanomaterial that has attracted extensive studies in recent years. In addition to its outstanding optical properties, low toxicity, high aqueous solubility and good biocompatibility [1-6] are prominent features that have turned it into a tough rival for other semiconductor quantum dots. Fabrication of CNPs is usually classified into two major approaches, top-down and bottom-up. Electrochemical oxidation [7-10], chemical oxidation [11] and laser ablation [12-25] are the most common proposed top-down methods to obtain CNPs from a carbonic source such as amorphous carbon [12], carbon black [20], multi-wall carbon nanotube [11], graphite [13,

17], bagasse [23] and agricultural waste [26]. Among them, a laser ablation method is a physical approach that employs a laser to fracture carbon bonding of a carbonic target embedded in gas [12-14, 25] or liquid [15-24] environment. Recent reports indicate that photoluminescence (PL) emission of CNPs synthesized by physical methods will be observed only after surface passivation [13, 27-30]. Hu and coworkers [16] suggested laser ablation of carbon materials in organic solvents, which leads to both synthesis and surface passivation in one step. As a result, laser ablation in a liquid is known as a green, low cost, and easy approach to produce fluorescent CNPs. There are remarkable research on the synthesis of CNPs using this method, with a focus on size control [17, 21, 22], PL efficiency [15-17, 24], optical nonlinearity [23], and structural properties [18-20]. Photoluminescence is strongly influenced by laser parameters. In the millisecond pulse regime, PL efficiency decreases significantly by increasing the pulse duration [17]. Moreover, irradiation time and laser pulse energy can have a positive effect on PL intensity [15]. PL emission spectra of CNPs are usually broad and the peak position depends upon the excitation wavelength. Three possibilities are considered for this interesting feature to include the difference in the size of nanoparticles [17, 31], different emissive traps on the CNP surface [24], both of them [27], or an unknown mechanism [1].

As a step towards clarifying some of the PL aspects, we have investigated the effect of liquids on the PL properties of the synthesized CNPs. For this purpose, four different solvents were employed, and the products were characterized using "attenuated total reflection Fourier-transform infrared" (ATR-FTIR) spectroscopy and photoluminescence spectroscopy. According to the results and by considering the properties of solvents, we deeply investigated the effect of solvent parameters impact on the PL characters of CNPs. By choosing a proper solvent and adjusting the laser parameters, tuning the color of fluorescent CNPs would be possible that is a valuable achievement in practical applications.

II. EXPERIMENTAL PROCEDURES

To synthesize fluorescent CNPs, the experimental details described by Hu et al. [16] were followed and the liquids containing polymer chains were selected. A schematic of the setup is shown in Fig.1. Four transparent solvents, polyethylene glycol, diethanolamine, diethylamine, and ethylenediamine were used as liquid platforms together with graphite powder (2 μm average size and with a concentration of 200 mg in 5 milliliter of solution in a stirrer with a speed of 15 rpm for 20 minutes) dispersed in the liquids as the carbonic source. A pulsed Nd:YAG laser at fundamental mode (1064 nm) with 10 ns pulse durations and 5 pulse repetition rate was employed to ablate the graphite for 1 hour. The laser pulse energy was 200 mJ and the ablated area was 15 mm2. A magnetic plate is used to make a homogenous solvent during the laser irradiation.

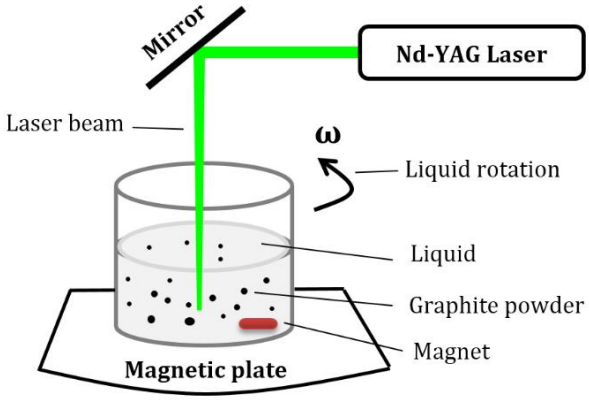

Fig. **1** Schematic of the experimental setup for CNP synthesis using a laser ablation method in liquid.

After a few hours, graphite powder was precipitated and a colorful supernatant that included CNPs was separated. Obtained CNPs in polyethylene glycol, diethanolamine, diethylamine, and ethylenediamine are shown in Fig. 2, labeled with samples A, B, C, and D, respectively.

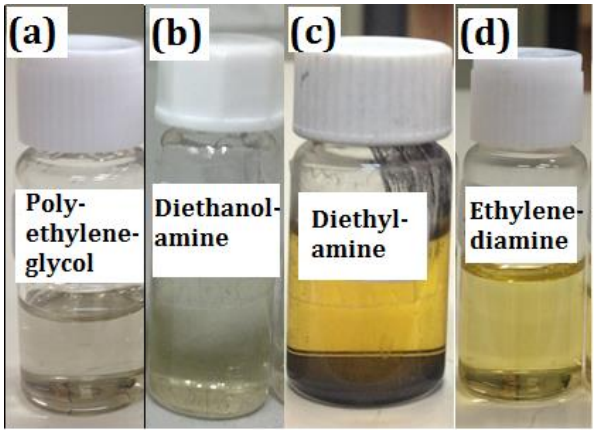

Fig. **2** CNP colloids synthesized in (a) polyethylene glycol, (b) diethanolamine, (c) diethylamine, and (d) ethylenediamine.

These four samples do not have the same colors. Sample C is an intense yellow suspension, however, it tends to transparent yellow in sample D. Sample B has pale yellow color and sample A is almost transparent. Since the color of colloids reflects the size of particles, the initial overview indicates that the smallest size of particles exists in sample A and the size becomes larger in other samples.

III. CHARACTERISTIC TECHNIQUES AND RESULTS

PL spectra of samples were measured at different excitation wavelengths to determine the effect of the liquid matrix. The results are shown in Fig. 3(a-d). Broad photoluminescence in the UV/Vis range is detected for all of the samples. Moreover, except for case D, the rest of the samples are excitation-wavelength dependence and redshift by decreasing the excitation energy. Moreover, CNPs in sample D exhibit a relatively narrow spectra and more intense PL compared to others. Also, a double emission PL is observed for all samples except sample C. The peak position of this double emission is not the same in different samples

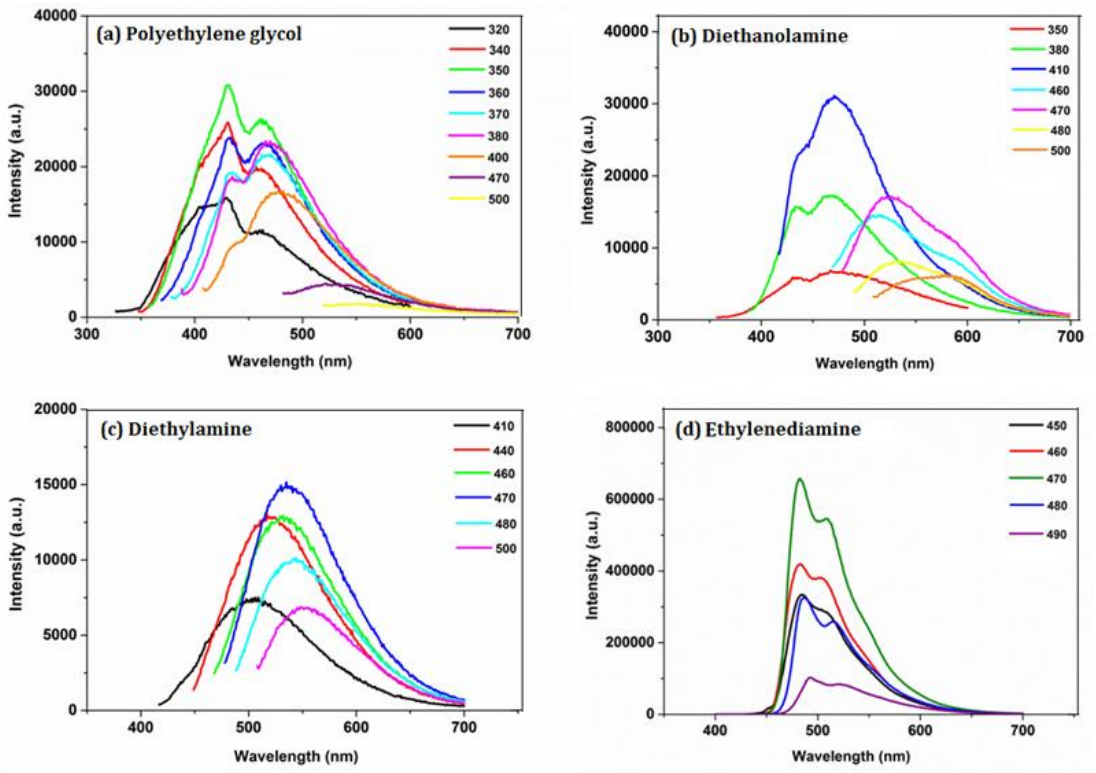

Fig. **3** PL spectra of the sample (a) A, (b) B, (c) C, and (d) D for different excitation wavelengths from 320 to 500 nm. The intervals around the maximum PL intensity are selected smaller to determine the exact location of the maximum emission intensity.

During the laser ablation process, a plasma plum is generated around the laser beam, which is due to the existence of high temperature and high-pressure conditions. After the condensing state and formation of CNPs, the surface of CNPs reacts with the -O-H, -O, -C-H, and -N-H chains that are fragmented molecular species of solvents [16]. To investigate the effect of surface emissive traps on the PL characteristics of CNPs in our experiment, ATR-FTIR spectroscopy was employed. Fig. 4 shows the surface functional groups of CNPs in sample A-D. Dynamic light scattering (DLS) measurement was also used to estimate the size of particles in each sample. As seen in Fig.5, CNPs in sample A with a large distance from others, at around 1 nm, have the smallest size and sample D includes the largest particles, at the average diameter of roughly 68 nm. CNPs in samples B and C are overall in the same order with a diameter of 37.8 nm.

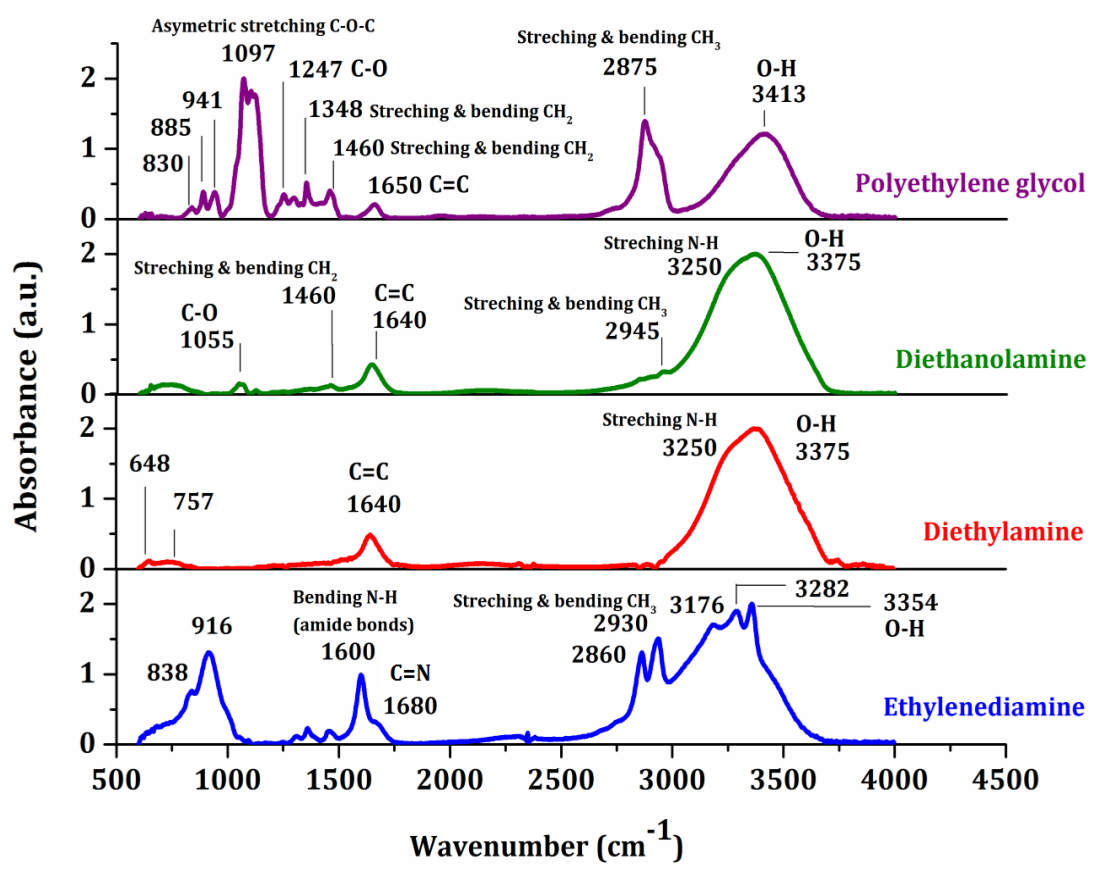

Fig. **4** ATR-FTIR spectra of CNP colloids synthesized (a) polyethylene glycol, (b) diethanolamine, (c) diethylamine, and (d) ethylenediamine.

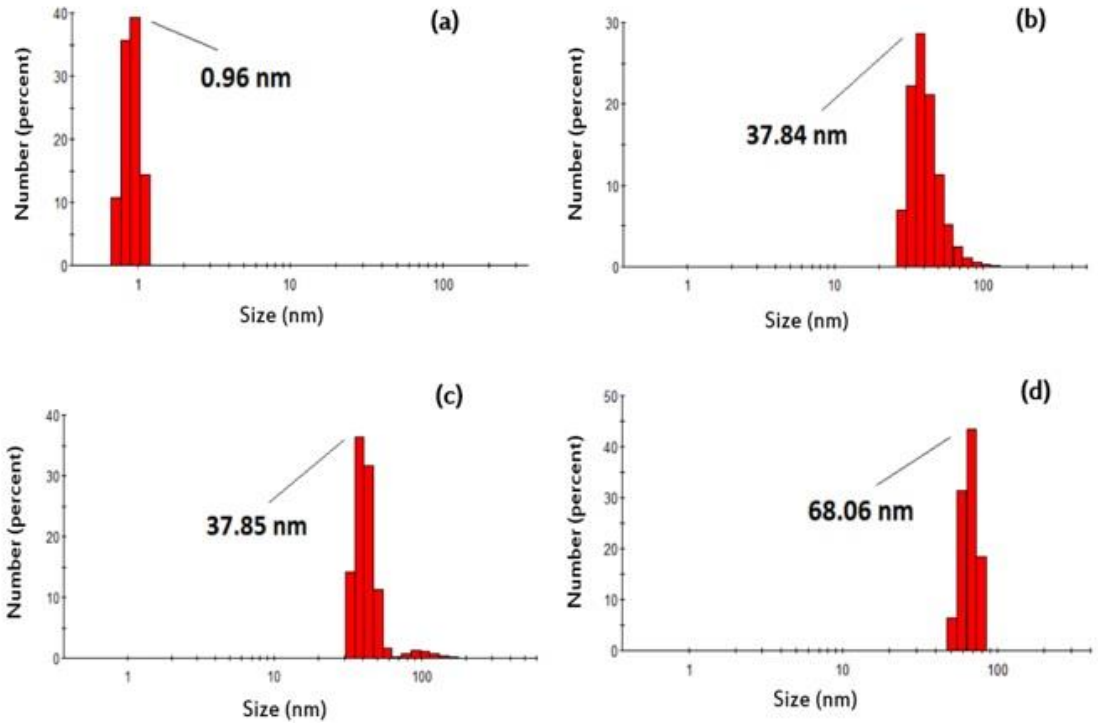

Fig. **5** DLS measurement and size distribution of CNPs in (a) polyethylene glycol, (b) diethanolamine, (c) diethylamine and, (d) ethylenediamine.

IV. DISCUSSION

Photoluminescence spectra of fig. 3 contain valuable information. The first key feature in fig. 3 shows that all of the spectra are excitation dependent other than sample D. Regarding the fact that CNPs synthesized in ethylenediamine have more surface functional groups compared to other samples (Fig. 4), the hypothesis that abundant surface chemical chains are responsible for PL excitation dependency [32] is excluded. Therefore, it seems that in sample D, the synergy effect [33] of functional groups is responsible for the narrow and excitation-independent PL spectrum. ATR-FTIR of sample D in our experiment shows a weak peak around 1680 cm-1 that is related to C=N bond, Moreover, two intense peaks around 916 and 838 cm-1 are related to the ring C-C-N and ring C-N-C bending vibration. The presence of these overlapped peaks together with the C=N bond eliminates the effect of broad and excitation-dependence PL of O-states and enhances the effect of Nitrogen atoms, which leads to an excitation-independent PL spectrum. To compare the peak position of PL spectra, the excitation and emission wavelengths are listed in Table 1. The excitation wavelength of maximum intensity is considered for each sample.

Table 1 PL emission and excitation wavelengths for samples A-D.

Sample	Excitation wavelength (nm)	1st PL wavelength (nm)	2nd PL wavelength (nm)
A	350	432	461
B	410	433	471
C	470	-	535
D	470	482	509

Three visible emissions, violet, blue, and green, are observed in Table 1. PL mechanism is assigned to the radiative recombination of localized electron-hole pairs that leads to a blue peak at around 475 nm [34], or emission from excited surface states. For the latter, because of the distinct energy distribution of surface states, each one can be excited with a specific range of wavelengths. For instance, for the C-O bond this excitation wavelength range is between 300-380 nm which causes an emission with a wavelength around 430 nm [24]. On the other hand, other functional groups, such as C=N, may influence on the energy levels of CNPs and shift this peak to longer wavelengths [32]. Therefore, violet and blue emissions in sample A and B, and a redshift to blue and green wavelength in sample D suggests the existence of C-O bonds in sample A and B, and the presence of additional functional groups in sample D, which C-O (1055, 1247 cm^{-1}) and C-O-C (1097 cm^{-1}) vibrations presented at ATR-FTIR spectra of sample A and B and carbon-nitrogen bonds in sample D (Fig. 4) also confirms that. Moreover, since no O or N functional groups are seen in ATR-FTIR of sample C, the only mechanism for the presence of a peak around 535 nm in its PL spectrum is electron-hole recombination.

Despite the same surface states in samples A and B, a small difference in their PL peaks position is observed that is likely due to the size confinement effect [17, 31] or molecular weight of solvents [16]. Based on the former hypothesis, PL wavelength undergoes a blue shift for smaller particles. On the other hand, according to the characteristic results of CNPs synthesized in Polyethylene glycol (PEG) with different molecular weight and almost constant size distribution, Hu et al. [16] suggested that the molecular weight of the solvent has a distinct effect on the PL peak position, and for mono size particles, increasing the molecular weight redshifts the PL peak to the longer wavelengths at maximum absorption excitation. In our experiment, regarding the DLS results (Fig. 5), the average size of CNPs in samples A, B are estimated to be 0.96 and 37.84 nm, respectively. Moreover, the properties of the solvents, including molecular weight, are also represented in Table 2.

Table 2 Linear chemical formula and properties of solvents in samples A-D.

Sample	Liquid	Chemical formula	Molecular weight of liquid (g/mol)	pH
A	Polyethylene glycol	$HO(C_2H_4O)_nH$	200	4-7
B	Diethanolamine	$(CH_2CH_2OH)_2NH$	105.1	11
C	Diethylamine	$(C_2H_5)_2NH$	73.1	13
D	Ethylenediamine	$NH_2CH_2CH_2NH_2$	60.1	12

From tables 1 and 2, sample B with lower molecular weight and larger particle size has a redshift in the peak position of PL compared to samples A. It is evident that in our experiment, in the competition between molecular weight and particle size, size is a determinative factor. However, it seems a fair suggestion that in the laser ablation method, molecular weight and particle size are not independent factors. In a colloid, large molecules can efficiently surround a CNP and prevent the carbon atoms aggregation. Moreover, the protective layer around the CNPs limits the growth of particles involved in the growth process. Therefore, if a liquid contains large molecules, the size of CNPs stays small in the initial stages of nucleation. Considering the DLS and molecular weight results in Table 2, this trend can be seen here. As a result, the first key factor that impacts on the PL peak position is the solvent components that create chain surface states on the CNPs. Secondly, particle size can contribute to a small shift in the PL spectra that is, in itself, determined by the molecular weight of the solvent.

It is reported that in chemical methods the intensity of PL peaks is sensitive to the pH of the solvent [32, 34]. Here we compare samples A and B that CNPs have almost the same surface states, but are produced in acid and base matrix, respectively. From Fig. 3, both spectra follow the same pattern. Although dual emission in sample A (B) is excitation dependent, they are locked on 432 (433) and 471 (461) nm for the excitation wavelengths below 400 nm. For larger wavelengths, we observe a redshift in the peak positions. Moreover, at short excitation wavelengths, the intensity of the first peak is dominant, however, the second one overcomes at larger excitation wavelengths. This alteration in dominant emission is likely due to the periodic excitation of surface states by changing the excitation wavelength [24]. The only difference is the ratio of violet to blue emission at the excitation wavelength with maximum intensity, which is larger than 1 in sample A but it is reverse in case B. Therefore, providing the same condition, a base liquid can increase the intensity of blue emission. Finally, from Fig. 3 it is evident that regarding the photoluminescence intensity, sample D is at the first level. It is also reported in other methods that Ethylenediamine is used as a surface passivation agent due to its high quantum yield [35]. From Fig. 4, N-H bending at around 1600 cm^{-1} and N-H stretching at 3100-3500 cm^{-1} show the track of amide groups on the surface of CNPs and are suspected to be responsible for the high photoluminescence of this sample.

V. CONCLUTION

In this research, fluorescent CNPs tunable in UV and visible ranges were synthesized by pulsed laser ablation technique of graphite target in four different liquids. PL spectra of surface passivated CNPs confirm the presence of fluorescent particles in products. ATR-FTIR results suggest that the appearance of strong photoluminescence is due to amide attachment on the surface of CNPs. Moreover, O-states on the CNPs surface lead a broad and excitation-dependent PL and the existence of Nitrogen atoms decrease the spectrum width and cause an excitation-independent PL. Also, by providing uniform surface states, a base liquid enhances aqueous diffusion. Particle size also affects the position of the PL peak, although it is not as important as the size of liquid components, as it is influenced by other criteria such as solvent molecular weight.

Acknowledgment

The authors are thankful to financial supports from Iran Polymer and Petrochemical Institute for grant No. 955801 dated 5th December 2016.

REFERENCES

[1] H. Li, Z. Kang, Y. Liu, and S.-T. Lee, "Carbon nanodots: synthesis, properties and applications," J. Mater. Chem, vol. 22, pp. 24230 (1-24), 2012.

[2] P. Namdari, B. Negahdari, and A. Eatemadi, "Synthesis, properties and biomedical applications of carbon-based quantum dots: An updated review," Biomedicine & Pharmacotherapy, vol. 87, pp. 209-222, 2017.

[3] R. Wang, K.-Q. Lu, Z.-R. Tang, and Y.-J. Xu, "Recent progress in carbon quantum dots: synthesis, properties and applications in photocatalysis," Journal of Materials Chemistry A, vol. 5, pp. 3717-3734, 2017.

[4] S. Y. Lim, W. Shen, and Z. Gao, "Carbon quantum dots and their applications," Chemical Society Reviews, vol. 44, pp. 362-381, 2015.

[5] D. L. Zhao and T.-S. Chung, "Applications of carbon quantum dots (CQDs) in membrane technologies: A review," Water research, vol. 147, pp. 43-49, 2018.

[6] R. Das, R. Bandyopadhyay, and P. Pramanik, "Carbon quantum dots from natural resource: A review," Materials today chemistry, vol. 8, pp. 96-109, 2018.

[7] J. Deng, Q. Lu, N. Mi, H. Li, M. Liu, M. Xu, L. Tan, Q. Xie, Y. Zhang, and Sh. Yao, "Electrochemical synthesis of carbon nanodots directly from alcohols," Chemistry–A European Journal, vol. 20, pp. 4993-4999, 2014.

[8] M. Liu, Y. Xu, F. Niu, J. J. Gooding, and J. Liu, "Carbon quantum dots directly generated from electrochemical oxidation of graphite electrodes in alkaline alcohols and the applications for specific ferric ion detection and cell imaging," Analyst, vol. 141, pp. 2657-2664, 2016.

[9] H. Ming, Z. Ma, Y. Liu, K. Pan, H. Yu, F. Wang, Z. Kang, "Large scale electrochemical synthesis of high quality carbon nanodots and their photocatalytic property," Dalton Transactions, vol. 41, pp. 9526-9531, 2012.

[10] J. Lu, J.-x. Yang, J. Wang, A. Lim, S. Wang, and K. P. Loh, "One-pot synthesis of fluorescent carbon nanoribbons, nanoparticles, and graphene by the exfoliation of graphite in ionic liquids," ACS nano, vol. 3, pp. 2367-2375, 2009.

[11] P. Saheeda, K. Sabira, J. Joseph, and S. Jayaleksmi, "Green chemistry route to realize, high quantum yield carbon quantum dots for cellular imaging applications," Materials Research Express, vol. 6, pp. 075025 (1-10), 2019.

[12] A. Sidorov, V. Lebedev, A. Kobranova, and A. Nashekin, "Formation of carbon quantum dots and nanodiamonds in laser ablation of a carbon film," Quantum Electronics, vol. 48, pp. 45-48, 2018.

[13] F. Kazemizadeh, R. Malekfar, and P. Parvin, "Pulsed laser ablation synthesis of carbon nanoparticles in vacuum," J. Phys. Chem. Solids, vol. 104, pp. 252-256, 2017.

[14] Y. Suda, T. Ono, M. Akazawa, Y. Sakai, J. Tsujino, and N. Homma, "Preparation of carbon nanoparticles by plasma-assisted pulsed laser deposition method—size and binding energy dependence on ambient gas pressure and plasma condition," Thin Solid Films, vol. 415, pp. 15-20, 2002.

[15] X. Li, H. Wang, Y. Shimizu, A. Pyatenko, K. Kawaguchi, and N. Koshizaki, "Preparation of carbon quantum dots with tunable photoluminescence by rapid laser passivation in ordinary organic solvents," Chem. Commun. vol. 47, pp. 932-4, Jan 21 2011.

[16] S.-L. Hu, K.-Y. Niu, J. Sun, J. Yang, N.-Q. Zhao, and X.-W. Du, "One-step synthesis of fluorescent carbon nanoparticles by laser irradiation," J. Mater. Chem. vol. 19, pp. 484-488, 2009.

[17] S. Hu, J. Liu, J. Yang, Y. Wang, and S. Cao, "Laser synthesis and size tailor of carbon quantum dots," J. Nanopart. Res., vol. 13, pp. 7247-7252, 2011.

[18] S. Hu, Y. Guo, Y. Dong, J. Yang, J. Liu, and S. Cao, "Understanding the effects of the structures on the energy gaps in carbon nanoparticles from laser synthesis," Journal of Materials Chemistry, vol. 22, pp. 12053-12057, 2012.

[19] S. Hu, Y. Guo, W. Liu, P. Bai, J. Sun, and S. Cao, "Controllable synthesis and Photoluminescence (PL) of amorphous and crystalline carbon nanoparticles," Journal of

Physics and Chemistry of Solids, vol. 72, pp. 749-754, 2011.

[20] S. Hu, Y. Dong, J. Yang, J. Liu, and S. Cao, "Simultaneous synthesis of luminescent carbon nanoparticles and carbon nanocages by laser ablation of carbon black suspension and their optical limiting properties," Journal of Materials Chemistry, vol. 22, pp. 1957-1961, 2012.

[21] H. P. S. Castro, V. S. Souza, J. D. Scholten, J. H. Dias, J. A. Fernandes, F. S. Rodembusch, R. dos Reis, J. Dupont, S. R. Teixeira, and R. R. B. Correia, "Synthesis and characterisation of fluorescent carbon nanodots produced in ionic liquids by laser ablation," Chemistry–A European Journal, vol. 22, pp. 138-143, 2016.

[22] V. Nguyen, L. Yan, J. Si, and X. Hou, "Femtosecond laser-induced size reduction of carbon nanodots in solution: Effect of laser fluence, spot size, and irradiation time," Journal of Applied Physics, vol. 117, pp. 084304 (1-6), 2015.

[23] D. Tan, Y. Yamada, S. Zhou, Y. Shimotsuma, K. Miura, and J. Qiu, "Carbon nanodots with strong nonlinear optical response," Carbon, vol. 69, pp. 638-640, 2014.

[24] V. Nguyen, J. Si, L. Yan, and X. Hou, "Direct demonstration of photoluminescence originated from surface functional groups in carbon nanodots," Carbon, vol. 108, pp. 268-273, 2016.

[25] H. Asano, S. Muraki, H. Endo, S. Bandow, and S. Iijima, "Strong magnetism observed in carbon nanoparticles produced by the laser vaporization of a carbon pellet in hydrogen-containing Ar balance gas," J. Phys.: Condens. Matter, vol. 22, pp. 334209, 2010.

[26] H. Baweja and K. Jeet, "Economical and green synthesis of graphene and carbon quantum dots from agricultural waste," Materials Research Express, 2019.

[27] Y.-P. Sun, B. Zhou, Y. Lin, W. Wang, K. A. Shiral Fernando, P. Pathak, M. J. Meziani, B. A. Harruff, X. Wang, H. Wang, P. G. Luo, H. Yang, M. E. Kose, B. Chen, L. M. Veca, S.-Y. Xie, "Quantum-sized carbon dots for bright and colorful photoluminescence," J. Am. Chem. Soc., vol. 128, pp. 7756-7757, 2006.

[28] L. Cao, X. Wang, M. J. Meziani, F. Lu, H. Wang, P. G. Luo, Y. Lin, B. A. Harruff, L. M. Veca, D. Murray, S.-Y. Xie, and Y.-P. Sun, "Carbon dots for multiphoton bioimaging," J. Am. Chem. Soc. vol. 129, pp. 11318-11319, 2007.

[29] Y.-P. Sun, X. Wang, F. Lu, L. Cao, M. J. Meziani, P. G. Luo, L. Gu, and L. Monica Veca, "Doped carbon nanoparticles as a new platform for highly photoluminescent dots," J. Phys. Chem. C, vol. 112, pp. 18295-18298, 2008.

[30] S.-T. Yang, X. Wang, H. Wang, F. Lu, P. G. Luo, L. Cao, M. J. Meziani, J.-H. Liu, Y. Liu, M. Chen, Y. Huang, and Y.-P. Sun, "Carbon dots as nontoxic and high-performance fluorescence imaging agents," J. Phys. Chem. C, vol. 113, pp. 18110-18114, 2009.

[31] Q.-L. Zhao, Z.-L. Zhang, B.-H. Huang, J. Peng, M. Zhang, and D.-W. Pang, "Facile preparation of low cytotoxicity fluorescent carbon nanocrystals by electrooxidation of graphite," Chem. Commun., pp. 5116-5118, 2008.

[32] H. Nie, M. Li, Q. Li, S. Liang, Y. Tan, L. Sheng, W. Shi, and S. Xiao-An Zhang, "Carbon dots with continuously tunable full-color emission and their application in ratiometric pH sensing," Chemistry of Materials, vol. 26, pp. 3104-3112, 2014.

[33] Y. Dong, H. Pang, H. B. Yang, C. Guo, J. Shao, Y. Chi, C. M. Li, and T. Yu, "Carbon-based dots co-doped with nitrogen and sulfur for high quantum yield and excitation-independent emission," Angewandte Chemie International Edition, vol. 52, pp. 7800-7804, 2013.

[34] O. e. Kozák, K. K. R. Datta, M. Greplová, V. c. Ranc, J. Kašlík, and R. Zbořil, "Surfactant-derived amphiphilic carbon dots with tunable photoluminescence," The Journal of Physical Chemistry C, vol. 117, pp. 24991-24996, 2013.

[35] W.-J. Niu, Y. Li, R.-H. Zhu, D. Shan, Y.-R. Fan, and X.-J. Zhang, "Ethylenediamine-assisted hydrothermal synthesis of nitrogen-doped carbon quantum dots as fluorescent probes for sensitive biosensing and bioimaging," Sensors and Actuators B: Chemical, vol. 218, pp. 229-236, 2015.

THIS PAGE IS INTENTIONALLY LEFT BLANK.